



Anticancer Activity against Brain Cancer Using Ni (II), Cu (II), Pd (II) and Au (III) Complexes Derived from Novel Mannich Base

Tamara Q. Manhee^{1*}, Ammar J. Alabdali²

^{1,2}Department of Chemistry, College of Sciences, Al-Nahrain University, Baghdad, Iraq

*Corresponding author: Tamara Q. Manhee, Department of Chemistry, College of Sciences, Al-Nahrain University, Baghdad, Iraq, Email: Tamaraqmanhee93@gmail.com

Submitted: 16 February 2023; Accepted: 17 March 2023; Published: 10 April 2023

ABSTRACT

New four metal ion complexes of Ni(II), Cu(II), Pd(II) and Au(III) were derived from the tridentate ligand 3-((3-(4-hydroxyphenyl)-5-mercapto-4H-1,2,4-triazol-4-yl)amino)benzofuran-2(3H)-one (L), which synthesized using condensation reaction of formaldehyde, acetone and secondary amine (Mannich reaction). The secondary amine is a heterocyclic compound possesses two rings. The structures of the new compounds and metal ion complexes were characterized using elemental analysis (C.H.N.S), FT-IR, UV-Vis spectroscopy, thermal gravimetric analysis (TGA), flame atomic absorption, molar conductivity and magnetic susceptibility measurements. Accordingly, the probable geometries of these complexes were suggested as square planner and all complexes were found to be of electrolytic nature. Thus, chemical formula; [NiLCI] Cl.6H₂O, [CuLCI]Cl.H₂O, [PdLCI]Cl.2H₂O and [AuLCI]Cl₂.3H₂O. Cytotoxic effect studding was applied on brain cancer cell line (AMJM) at using the MMT method for complexes and L. Gold (III) complex has the highest cytotoxicity among all tested compounds.

Keywords: Mannich Base, intermolecular cyclization, Ni(II), Cu(II), Pd(II), Au(III) Complexes

INTRODUCTION

In the beginning of 1950s, coordination chemistry field occupied large area of chemistry science for its fast in the development of the practical aspect in the preparation of complexes, in addition to contribution in the knowledge of complexes of structures [1]. These complexes playing significant an increasing role in various areas: industry, agriculture and medicine [2, 3]. The production of metal complexes is phenomenon which is not confined only to transition elements, but also for represented elements [4] and observed especially in the transition elements as it provides an empty orbitals with suitable energy of nonmetal atoms

orbital of ligands whether organic, inorganic, or ions that have nonbonding pair of electrons [3]. Bioinorganic chemistry is a branch acts as a bridge between biochemistry and inorganic chemistry and tries to describe the role of inorganic constituents in biochemical processes [5]. Biomolecules that possess one or more metallic elements can be called metallobiomolecules that are natural products and usually complex coordination compounds. The active sites (metal sites) are generally contained the various biochemical processes such as electron transfer, binding of exogenous molecules and catalysis [6].

Several N-heterocyclic compounds found in nature, have physiological and pharmacological activities and they are components of a wide variety of physiologically essential molecules, including several vitamins, nucleic acids, medicines, antibiotics, dyes, and agrochemicals [7, 8]. Additionally, they are a component of a large number of pharmacologically active compounds [9]. DNA and RNA base pairs (guanine, cytosine, adenine, and thymine) are also composed of N-heterocyclic chemicals, such as purines and pyrimidine [10]. Heterocyclic compounds are a class of organic chemicals that are medicinally useful. In addition, fused ring heterocyclic constitute a significant component of a number of currently accessible medicinal medicines. Heterocyclic aromatic compounds occur naturally in a broad variety of animal and plant tissues [11]. Triazole, also called pyrotriazole, is a type of organic heterocyclic compound with a five-membered unsaturated ring structure consisting of three nitrogen atoms and two carbon atoms in non-adjacent locations, the name of triazole was first given by Bladin in 1885 [12]. Triazoles are crystalline substances that range in color from white to light yellow and are soluble in both water and alcohol, it shows high aromatic stabilization compared to other organic compounds [13]. Triazole nucleus stabilized by resonance, i.e., tautomeric forms occur in both triazole isomers. Triazole has two isomers (1,2,3-triazole and 1,2,4-triazole) with the chemical formula $C_2H_3N_3$ [14]. Mannich reactions are applied in organic syntheses of some natural compounds for example: peptide compounds, nucleotide compounds, alkaloid compounds and antibiotics. Mannich reactions are implied in the syntheses of medicinal compounds like rolitetracycline (Mannich base of tetracycline), fluoxetine (antidepressant), tramadol (analgesic) and tolmetin (anti-inflammatory) [15]. Mannich reaction

compounds application such as antihypertensive [16], antioxidant [17], anticancer [18] and antibacterial [19].

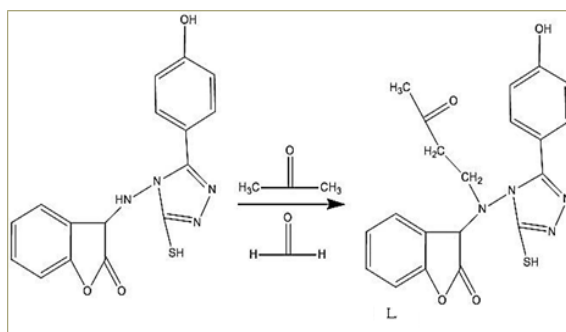
EXPERIMENTAL

Materials and instruments

The used reagents, starting materials and solvents were purchased commercially without any further purification. Melting points were determined using open capillary method on hot stage Gallenkamp melting point apparatus and were uncorrected. 1H -NMR and ^{13}C -NMR spectra were recorded on Bruker spectrophotometer model AV 400 Advance-III for 400 MHz in DMSO- d_6 solution with the TMS as internal standard. Infra-red spectra were recorded with FT-IR.8400s Shimadzu spectrophotometer at range (4000-200) cm^{-1} using CsI disks. The Ultra violet-Visible spectra were measured on Shimadzu UV-Vis. 1800 Ultra Violet Spectrophotometer in the range (190-1100) nm. Thermal analysis TGA was performed with (DSC1 STARE system) METTLER TOLEDO Co. The conductivity measuring of metal ion of all complexes was studied in 10^{-3} M DMSO which was determined in Hunts Capacitors. The metal content of the complexes were measured by using flame-atomic absorption technique by nova 350.

Syntheses

Mannich base was synthesized by three compound formaldehyde 0.01 mol, (0.3 gm), acetone 0.01 mol, (0.58 gm) and cyclic ester (3-((3-(4-hydroxyphenyl)-5-mercapto-4H-1,2,4-triazol-4-yl)amino)benzofuran-2(3H)-one) 0.01 mol, (3.96 gm) in ethanolic solution 15 mL. Then, the mixture was refluxed for 18 hours. A solid yellow compound was obtained, filtered, and washed with cold ethanol followed by petroleum ether. Then, the final product was dried [20, 21].



SCHEME 1: Synthesis successive steps to produce ligand (L)

Syntheses of complexes

Alcoholic solution of 0.001mol metal salts $\text{NiCl}_2 \cdot 2\text{H}_2\text{O}$, $\text{CuCl}_2 \cdot 6\text{H}_2\text{O}$, $\text{PdCl}_2 \cdot 2\text{H}_2\text{O}$ and $\text{HAuCl}_3 \cdot 3\text{H}_2\text{O}$ in weights 0.23gm, 0.13gm, 0.21gm and 0.39gm respectively dissolved in 10 mL absolute ethanol individually added to 0.001 mol (0.396gm) of L and dissolved in 8mL absolute ethanol. The mixtures were refluxed for 2 hrs, and then colored crystalline solid complexes were formed. The products were filtered and dried.

Cytotoxicity Assays

MTT cell viability assay was using 96-well that seeding accord at 1×10^4 cells/well plates. After one day or a confluent monolayer was achieved once, cells were treated with tested compounds. Cell viability was checked and measured after three days of treatment and adding 28 μL of 2 mg/mL solution of MTT then incubating the cells lines at 37 °C for one half hour. The remaining crystals in

the wells were solubilized in the addition of DMSO (130 μL) followed by incubation (37°C) for 15 mins and shaking [22]. Absorbency was determined at 492 nm test wavelength. The rate of inhibition of cell growth (the percentage) was calculated by using following equation. Inhibition rate = $(A-B)/A \times 100$

Where A was the control of optical density

Where B was the test of optical density

RESULTS AND DISCUSSION

The importance of preparing Mannich base compound arises from their versatility as starting materials for the synthesis of many compounds. The structures of the prepared Mannich base with its metal ion complexes were identified by using different techniques. Compound was synthesized as described in Scheme 1 and the physical properties of synthesized compounds with metal content are listed in Table 1.

TABLE 1: The physical properties of synthesized compounds

Com	M. Wt g.mol ⁻¹	Yield d%	Color	M.P (°C)	Micro elemental analysis calc. (Found)					M % Cal (Found)	Cl % Cal (Found)
					C%	H%	N%	S%	O%		
L	410.45	72	Yellow	220-222	58.53 (58.66)	4.38 (4.98)	13.64 (13.61)	7.79 (7.57)	15.72 (15.18)	-----	-----
C ₁	648.16	70	Pall-Brown	300 Decompose	40.11 (39.21)	4.62 (4.39)	8.63 (8.49)	4.93 (4.61)	24.68 (22.84)	9.05 (8.95)	10.93 (10.00)
C ₂	580.93	76	Green	290-292	41.31 (40.53)	3.78 (3.88)	9.63 (9.22)	5.50 (5.61)	17.26	10.93 (10.65)	12.20 (13.09)

									(16.52)		
C ₃	623.45	88	Brown	345-347	38.49 (36.89)	3.52 (3.97)	8.98 (8.22)	5.13 (5.18)	15.39 (15.69)	17.06 (16.97)	11.37 (11.91)
C ₄	804.28	82	Reddish-Orange	350 Decompose	29.84 (28.63)	3.10 (3.27)	6.96 (6.66)	3.97 (3.37)	13.92 (13.67)	24.49 (24.21)	17.63 (17.78)

Infrared spectroscopy

The absorption bands of synthesized compounds are listed along with some characteristic peaks in Table 2.

3-((3-(4-hydroxyphenyl)-5-mercapto-4H-1,2,4-triazol-4-yl) (2-oxopropyl) amino) benzofuran-2(3H)-one hydrate compound (L)

The infrared spectrum of compound (L) was shown the appearance of new characteristic band at 1702 cm⁻¹ which could be attributed to ν C=O group of ketone [23]. Furthermore the disappearance of ν N-H group indicated the formation of mannich base ligand (L).

FT-IR of the complexes (C1-C4)

The FT-IR spectra of these complexes C1-C4 that derived from L showed shifting of ν C=O group of ester to high frequency by the range 16-10 in the complexes appeared at (1826, 1822, 1827 and 1822) cm⁻¹ for (C1-C4) complexes respectively. Carbonyl of acetone (C=O) group of shifted to lower frequency at range 18-6 in the complexes appeared at (1693, 1686, 1691 and 1684) cm⁻¹ for C₁-C₄ respectively. Coordination of metal element bonding due to ν M-N, ν M-O and ν M-Cl bands were appeared at ranges (545-599, 455-491 and 368-381) cm⁻¹ respectively, that considers as further support for the coordination of ligand with metal ions [24, 25].

TABLE 2: The most important absorption bands of the synthesized ligand and complexes

Comp	C=O Ester	C=O acetone	ν (M-N)	ν (M-O)	ν (M-Cl)
L	1812	1702
C ₁	1826	1693	559	491	370
C ₂	1822	1686	545	455	368
C ₃	1872	1691	563	462	381
C ₄	1822	1684	599	491	378

Proton and carbon nuclear magnetic resonance spectroscopy (1H-NMR and 13C-NMR)

¹H-NMR has been used for characterization the new synthesized compounds. The spectrum of the ligand (L) showed a singlet signal at 2.3 ppm for the CH₃ group, A doublet signal at 4.66 ppm appeared for C-H group while singlet signal at 7.91 ppm for the O-H group. While for the aromatic group appeared as a multiplet in the range 6.88-7.91 ppm protons [26]. singlet signal at 13.9 ppm for the S-H group. ¹H-NMR spectra of the complexes showed a singlet signal at

(14.00, 13.84, 13.77 and 13.77) ppm for the S-H group for C₁-C₄ respectively. While for the aromatic group appeared as a multiplet in the ranges (6.54-7.71, 6.58-8.06, 6.57-7.67 and 6.55-8.01) ppm for C₁-C₄ respectively while singlet signal at (8.03, 8.08, 7.67 and 8.09) ppm for the O-H group for C₁-C₄ respectively. While the signal of CH₃ shifted to range (1.72-2.51) ppm. ¹H-NMR data were listed along with some characteristic peaks in Table 3. The ¹H-NMR spectra were shown in Figures (1-5).

TABLE 3: $^1\text{H-NMR}$ data of ligand L and metal ion complexes

Comp	δ S-H	δ C-H aromatic	δ O-H	δ C-H	δ CH ₂	δ CH ₃ proton
L	13.9, s	6.88-7.91, m	7.91, s	4.66, s	3.69, s	2.30, s
C ₁	14.00, s	6.54-7.71, m	8.03, s	4.66, s	2.58, s	1.72, s
C ₂	13.84, s	6.58-8.06, m	8.08, s	4.84, s	2.5, s	1.92, s
C ₃	13.77, s	6.57-7.67, m	7.67, s	4.76, s	2.81, s	2.51, s
C ₄	13.77, s	6.55-8.01, m	8.09, s	4.78, s	2.91, s	2.51, s

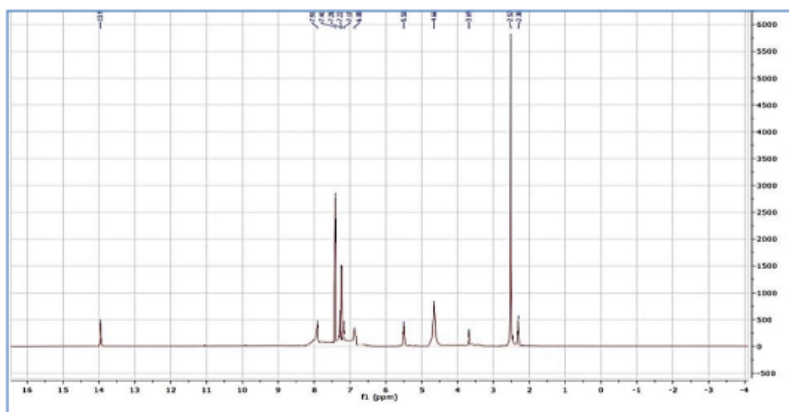


FIGURE 1: $^1\text{H-NMR}$ Spectrum of L

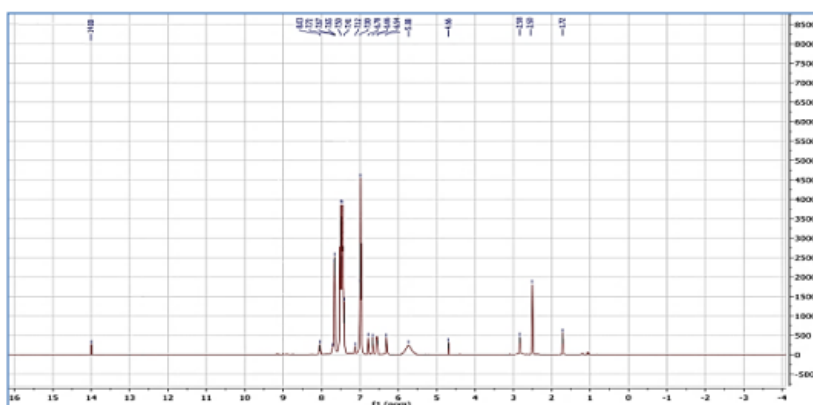


FIGURE 2: $^1\text{H-NMR}$ Spectrum of C₁ Complex

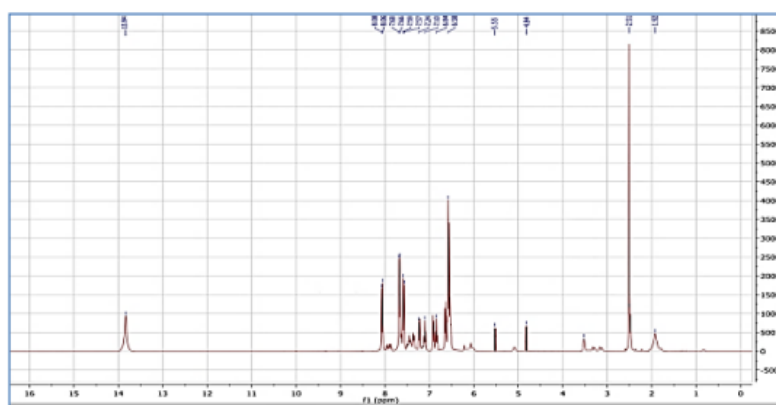


FIGURE 3: $^1\text{H-NMR}$ Spectrum of C₂ Complex

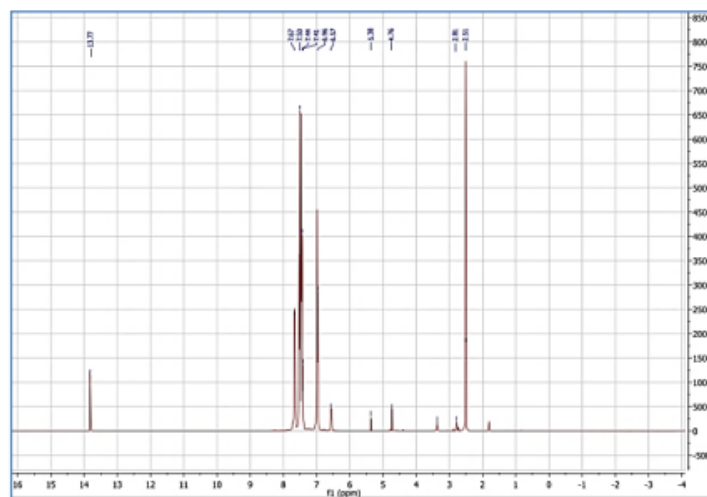


FIGURE 4: ¹H-NMR Spectrum of C₃ Complex

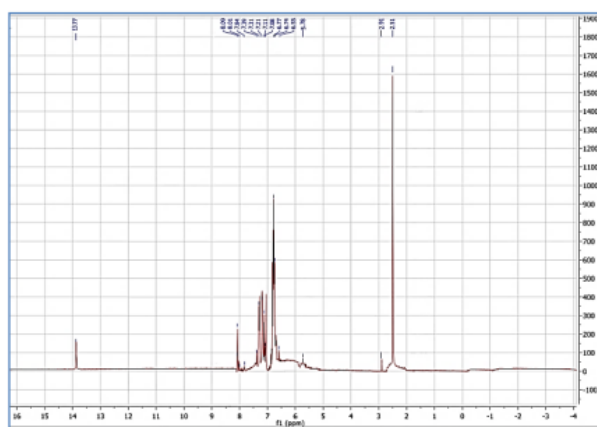


FIGURE 5: ¹H-NMR Spectrum of C₄ Complex

¹³C-NMR spectrum of ligand was showed several peaks the first one appeared at ~40 ppm and was corresponded to solvent DMSO, while the second appeared at 200 ppm corresponded to carbon of acetone C=O, peak at 170 ppm was corresponded to C=O of ester. The other peak appeared at 158 which corresponded to C-OH. The chemical shift of CH₂ appeared at δ 40 ppm. The chemical shift of (C-aromatic ring) appeared at δ 116-130 ppm. while chemical shifts of CH₃ appeared at δ 27 ppm [26]. The ¹³C-NMR spectra of the complexes C₁-C₄ showed peaks: was that the

signal of C=O carbon of acetone of the ligand was shifted in these complexes to range 203-204 ppm for C₁-C₄. The signal of C=O of ester in the prepared complexes appeared at 169 ppm. Another peaks were shown in the complexes at range 154-156 ppm refers to proton C-OH. While S-C=N of 1,2,4 triazole appeared at (169, 166, 167 and 165) for C₁-C₄ respectively. While CH₂ appeared at rang δ 40-41 ppm. Other peaks were shown appeared at δ 25 ppm refers to CH₃ of complexes (C₁-C₄). The ¹³C-NMR spectra were show in Figures (6-10).

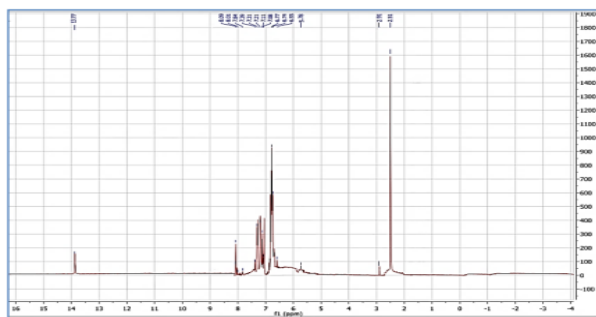


FIGURE 6: ¹³C-NMR Spectrum of L

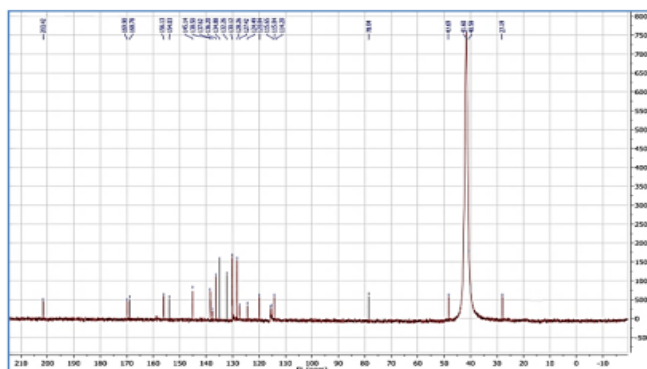


FIGURE 7: ¹³C-NMR Spectrum of C₁ Complex

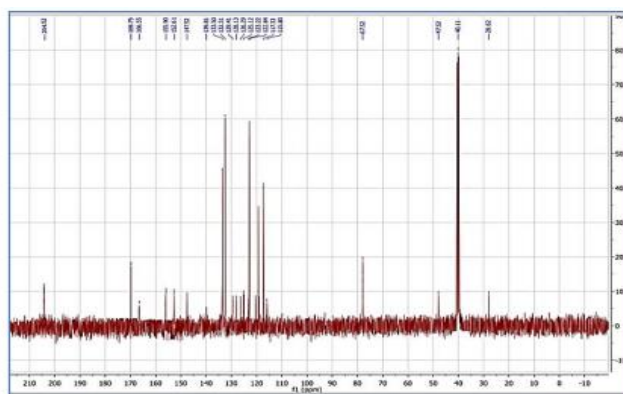


FIGURE 8: ¹³C-NMR Spectrum of C₂ Complex

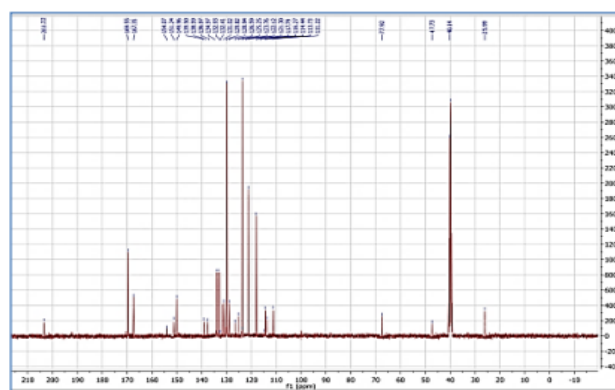


FIGURE 9: ¹³C-NMR Spectrum of C₃ Complex

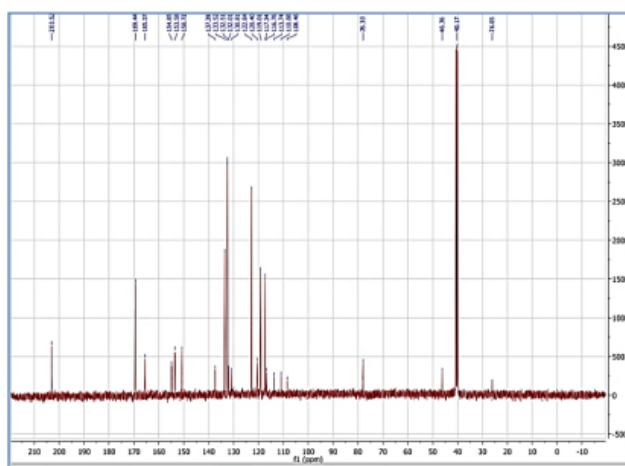


FIGURE 10: ^{13}C -NMR Spectrum of C_4 Complex

Thermal Studies

Thermogravimetric analysis TG of compound was performed to prove the suggested structures and study the thermal stability of the ligand and complexes. The run was tested at range 25-800 °C

of heating under nitrogen gas and rate 10°C/min. The decomposition temperature, mass loss percentage, and the residue present of the complexes are given in Table 4.

TABLE 4: Thermogravimetric analysis results for ligand and metal complexes

Comp.	Molecular formula	Step	Temp. rang of the Decomposition C°	Suggested Formula of loss	Mass loss%	
					Cal.	Found
L	$\text{C}_{20}\text{H}_{18}\text{N}_4\text{O}_4\text{S}$ 410.45	1	400-450	H_2S , $\text{C}_4\text{H}_8\text{O}$	25.85	25.97
		2	590-610	$\text{C}_8\text{H}_5\text{O}_2$	32.40	32.91
		3	610-630	$\text{C}_8\text{H}_5\text{N}_4\text{O}$	42.19	41.45
C_1	$[\text{Ni}(\text{L}_1)\text{Cl}] 6\text{H}_2\text{O}\cdot\text{Cl}$ 648.16	1	100-150	$6\text{H}_2\text{O}$, Cl_2	27.60	27.03
		2	300-350	H_2S , $\text{C}_4\text{H}_8\text{O}$	36.80	36.69
		3	600-650	$\text{NiC}_8\text{H}_5\text{N}_4\text{O}$	35.70	36.10
C_2	$[\text{Cu}(\text{L}_1)\text{Cl}] 2\text{H}_2\text{O}\cdot\text{Cl}$ 580.93	1	100-150	$6\text{H}_2\text{O}$, Cl_2	18.40	18.77
		2	200-300	H_2S	5.85	5.85
		3	400-500	$\text{C}_4\text{H}_8\text{O}$	12.33	11.22
		4	550-650	$\text{C}_8\text{H}_5\text{O}_2$	22.89	22.25
		5	700-750	$8\text{N}_4\text{OCuC}$	40.71	41.63
C_3	$[\text{Pd}(\text{L}_1)\text{Cl}] 2\text{H}_2\text{O}\cdot\text{Cl}$ 623.45	1	50-100	$2\text{H}_2\text{O}$, Cl_2	17.14	17.77
		2	200-300	H_2S , $\text{C}_4\text{H}_8\text{O}$	17.00	17.55
		3	300-350	$\text{C}_8\text{H}_5\text{O}_2$	58.16	22.22
		4	550-600	$8\text{N}_4\text{OCdP}$	44.81	43.35
C_4	$[\text{Au}(\text{L}_1)\text{Cl}] 3\text{H}_2\text{O}\cdot\text{Cl}_2$ 767.76	1	100-150	$3\text{H}_2\text{O}$, Cl_2 , HCl	20.83	20.52
		2	300-400	H_2S , $\text{C}_4\text{H}_8\text{O}$, $\text{C}_8\text{H}_5\text{O}_2$	30.34	30.77
		3	550-600	$8\text{N}_4\text{OCuA}$	48.18	48.43

Ultraviolet-visible spectroscopy, magnetic susceptibility and molar conductivity

The electronic spectrum of Ni (II) complex showed one band at 892 nm (11210 cm^{-1}) could

be attributed to d-d electronic transition which assigned to $^1\text{A}_{1g} \rightarrow ^1\text{B}_{1g}$ of square planer geometry [27, 28]. While complex of Cu (II) was show one band observed at 872 nm (11467 cm^{-1})

which can be assigned to ${}^2B_{1g} \rightarrow {}^2A_{1g}$ transition of square planer geometry [29-31]. The complex of Pd (II) was show one band at 700 nm (14285cm^{-1}) which could be assigned to ${}^1A_{1g} \rightarrow {}^1A_{2g}$ of square planer geometry [32, 33]. The last complex of Au(III) showed one band at (403 nm, 24813 cm^{-1}) which could be refer to charge transfer transitions of square planer geometry [34], Since the gold complex ion has a large size, it's in the third transition series and has a high oxidation state, the complexes have a high crystal field effect. Thus, the spectrum of such ion was characterized by a charge transfer band that dominates the ligand field transition. This mean

that the charge transfer bands appear at longer wavelength, at the same time ligand filed transition are expected to appear at shorter wavelength. These results in an overlap between the two absorption bands, which make the interpretation of the spectra more difficult [35, 36]. The molar conductance values of the synthetic complexes obtained in DMSO at 10^{-4}M as a solvent at room temperature. The electronic transitions data, magnetic properties and molar conductivity of the complexes were listed in table 5. The result showed for the complexes C_1 - C_3 1:1 electrolytic while C_4 was 1:2 electrolytic[37].

TABLE 5: Electronic spectra of the prepared complexes and ligand

Comp.	Wavelength $\lambda(\text{nm})$	Wave no. $\bar{\nu}$ (cm^{-1})	Assignment	Molar Cond. $\text{S.cm}^2\text{ molL}^{-1}$	μ eff (B.M)	Suggested Geometry
L	318	31446	$\pi \rightarrow \pi^*$
C_1 Ni(II)	897	11148	$1A_{1g} \rightarrow 1B_{1g}$	37	Di	Square planner
C_2 Cu(II)	810 703	12345	${}^2B_{1g} \rightarrow {}^2A_{1g}$ ${}^2B_{1g} \rightarrow {}^2E_g$	45	1.96	Square planner
C_3 Pd(II)	698	14326	${}^1A_{1g} \rightarrow {}^1A_{2g}$	36	Di	Square planner
C_4 Au(III)	385	25974	C.T	81	Di	Square planner

Cytotoxic effect of the ligand and complexes on AMJM cell line (MTT assay)

Firstly we investigated and compared the effects of the ligand and complexes on cancer cell growth. Human brain cancer (AMJM) cells were treated with L, C_1 , C_2 , C_3 and C_4 at different concentrations (6.125, 12.5, 25, 50 and 100) $\mu\text{g/mL}$ for 72 hrs, followed by 3-(4,5-dimethyltriazol-2-yl) -2,5diphenyltetrazolium bromide (MTT) colorimetric assay [38]. The cells were treated with the solvent DMSO which used as control. We found that ligands and complexes were growth-inhibitory potency in a dose dependent manner at most concentrations.

The main problem of cytotoxicity of many anticancer agents is partially effect due to the inability to distinguish between normal cells and tumor cells. We designed compounds for their primary anticancer assay (heterocyclic

group)[39]. In order to eliminate toxicity in normal cell, it is necessary to identify some specific properties of cancer cells different from normal cells [40], numerous transition metal complexes have been synthesized and screened for their anticancer properties [41]. Therefore, study the action of ligands and complexes to cancer cells. First of all, we measured the anti-proliferation activity of these ligand and complexes by the MTT assay, and found that most compounds in most concentrations have the ability to kill human brain cancer cells in a concentration-dependent manner. Aanticancer activity results present that ligand and complexes are active against brain cancer cell (AMJM). Moistly, the presence of nitrogen, oxygen and sulphur in the heterocyclic moieties in the ligand skeleton show diverse biological activity. Benzofuran and triazoleare important

heterocyclic compounds which show anticancer activity [42]. In addition the mannich base compound increases anticancer activity [43]. The result of anticancer activity show in Table 6 and Figures 11-15

TABLE 6: Cytotoxicity effect of prepared compounds on the AMJM tumour cell line

Comp.	IR%, (C) $\mu\text{g/mL}$	PR%, (C) $\mu\text{g/ML}$	Other effect cytotoxicity%, (C) $\mu\text{g/mL}$		
L	43 (100)	7 (12.5)	3 (6.125)	10 (25)	25 (50)
C ₁	57 (100)	32 (12.5)	22 (6.125)	37 (25)	42 (50)
C ₂	63 (100)	39 (12.5)	25 (6.125)	41 (25)	56 (50)
C ₃	70 (100)	38 (12.5)	35 (6.125)	43 (25)	61 (50)
C ₄	74 (100)	42 (12.5)	40 (6.125)	49 (25)	55 (50)

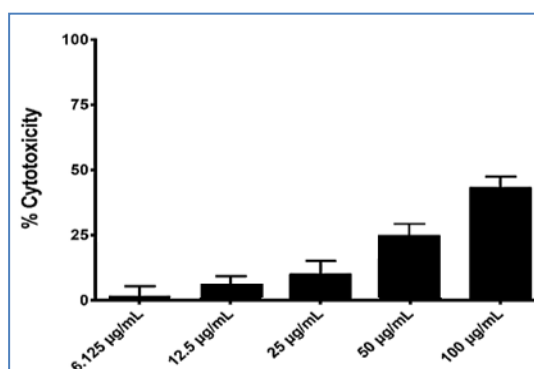


FIGURE 11: Cytotoxic effect of ligand L in AMJM

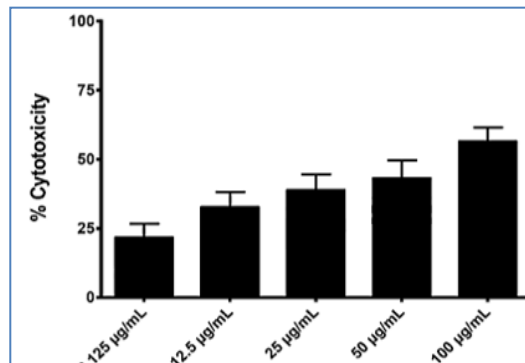


FIGURE 12: Cytotoxic effect of complex C₁ in AMJM

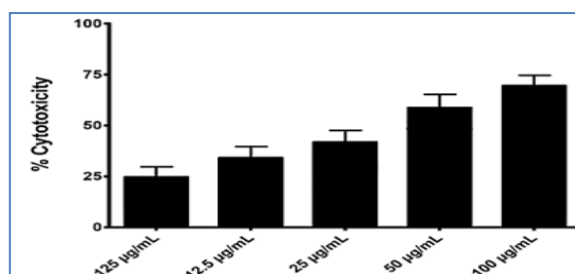


FIGURE 13: Cytotoxic effect of complex C₂ in AMJM

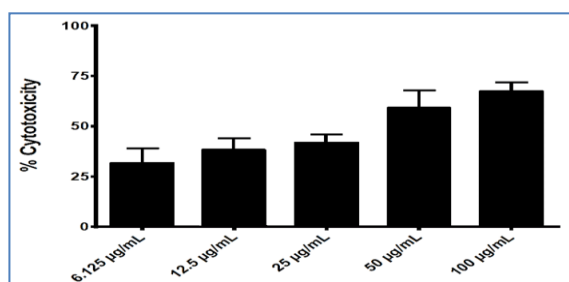


FIGURE 14: Cytotoxic effect of complex C₃ in AMJM

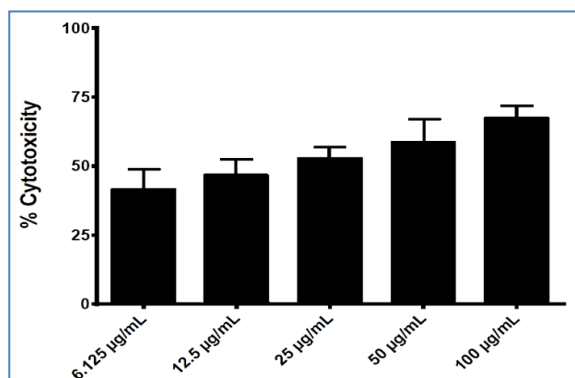


FIGURE 15: Cytotoxic effect of complex C₄ in AMJM

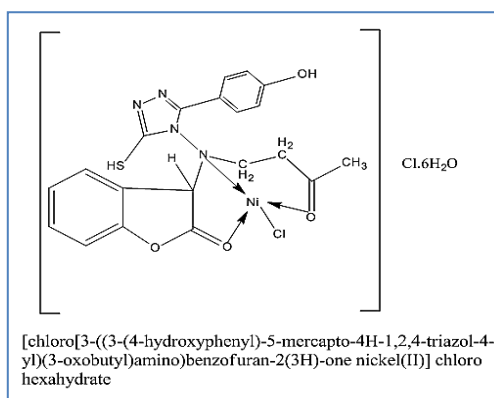


FIGURE 16: Suggested structure of [NiLCl]Cl.6H₂O complex (C₁)

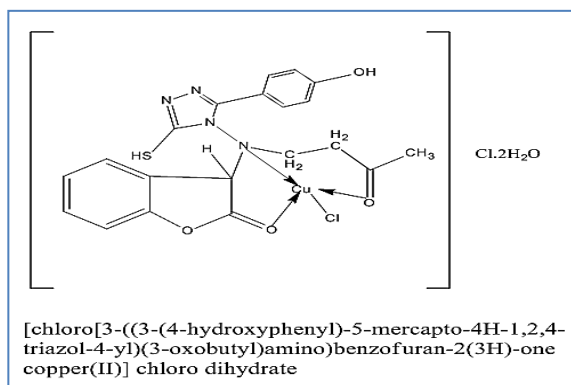


FIGURE 17: Suggested structure of [CuLCl]Cl.2H₂O complex (C₂)

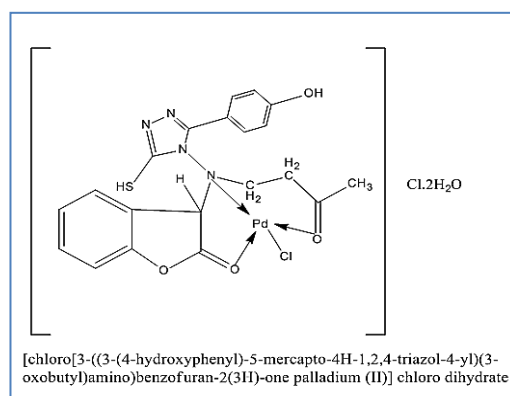


FIGURE 18: Suggested structure of [PdLCl]Cl₂.2H₂O complex (C₃)

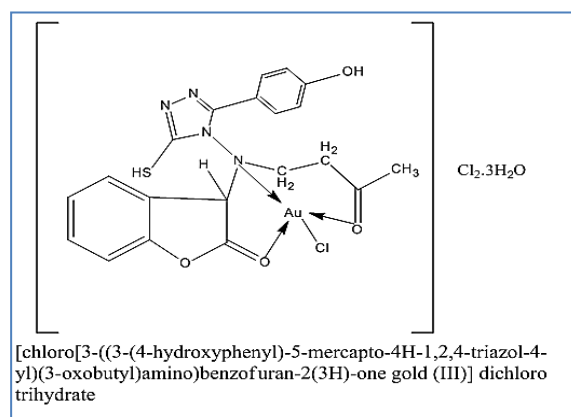


FIGURE 19: Suggested structure of [AuLCl]Cl₂.3H₂O complex (C₄)

CONCLUSIONS

In spite of ligand being multidentate with different donor atoms, the coordination was tridentate through two oxygen atoms and one nitrogen atom in as five membered ring form. The complexes of gold, palladium, nickel, and copper have square planer geometry of chemical formula: [NiLCl]Cl₂.6H₂O, [CuLCl]Cl₂.2H₂O, [PdLCl]Cl₂.2H₂O and [AuLCl]Cl₂.3H₂O respectively, all have chloride counter ion and have been hydrated salts (Figures 16-19). The MTT assay methods of selected ligand and complexes have shown significant cytotoxicity. Gold (III) complex has the higher value against the AMJM cell line among other complexes, values which are arranged as follows: Au(III) > Pd(II) > Cu(II) > Ni(II) > L. The high charge of gold (III) could be one of significance and may have played a role in the anticancer activity beside square planer geometry that resembling cisplatin.

REFERENCES

- Gispert, J.R., Coordination chemistry. Vol. 483. 2008: Wiley-VCH Weinheim.
- Farrell, N., Biomedical uses and applications of inorganic chemistry. An overview. Coordination Chemistry Reviews, 2002. 232(1-2): p. 1-4.
- Crabtree, R.H., The organometallic chemistry of the transition metals. 2009: John Wiley & Sons.
- Lyčka, A., et al., ²⁷Al, ¹⁵N, ¹³C and ¹H NMR spectra and negative-ion electrospray mass spectra of the 2: 1 aluminium (III) complexes of azo dyes derived from anthranilic acid. Dyes and pigments, 2001. 50(3): p. 203-209.
- Crichton, R. and R. Louro, Practical approaches to biological inorganic chemistry. 2019: Elsevier.
- Kaim, W., B. Schwederski, and A. Klein, Bioinorganic Chemistry--Inorganic Elements in the Chemistry of Life: An Introduction and Guide. 2013: John Wiley & Sons.
- Verma, C., et al., Pyridine based N-heterocyclic compounds as aqueous phase corrosion inhibitors: a review. Journal of the Taiwan

- Institute of Chemical Engineers, 2020. 117: p. 265-277.
- Goni, L.K., et al., Bioinspired heterocyclic compounds as corrosion inhibitors: a comprehensive review. *Chemistry—An Asian Journal*, 2021. 16(11): p. 1324-1364.
 - Maeng, S.K., et al., Occurrence and fate of bulk organic matter and pharmaceutically active compounds in managed aquifer recharge: a review. *Water Research*, 2011. 45(10): p. 3015-3033.
 - Omar, A., REVIEW ARTICLE; ANTICANCER ACTIVITIES OF SOME FUSED HETEROCYCLIC MOIETIES CONTAINING NITROGEN AND/OR SULFUR HETEROATOMS. *Al-Azhar Journal of Pharmaceutical Sciences*, 2020. 62(2): p. 39-54.
 - Hossain, M. and A.K. Nanda, A review on heterocyclic: synthesis and their application in medicinal chemistry of imidazole moiety. *Science*, 2018. 6(5): p. 83-94.
 - Ali, K. and A.S. Alimuddin, Short review on 1, 2, 4-Triazole with various pharmacological activity. *SD Int. J. Pharm. Sci*, 2018. 1(1): p. 14-22.
 - Zafar, W., S.H. Sumrra, and Z.H. Chohan, A review: pharmacological aspects of metal based 1, 2, 4-triazole derived Schiff bases. *European journal of medicinal chemistry*, 2021. 222: p. 113602.
 - Prasanna, C.A. and A. Sharma, Pharmacological Exploration of Triazole-based Therapeutics for Alzheimer's Disease: An Overview. *Current Drug Targets*, 2022. 23(9): p. 933-953.
 - Maria, K., H.-L. Dimitra, and G. Maria, Synthesis and anti-inflammatory activity of chalcones and related Mannich bases. *Medicinal chemistry (Sharjah (United Arab Emirates))*, 2008. 4(6): p. 586-596.
 - El-Gendy, A.A. and H.A. El-Banna, Synthesis and antihypertensive activity of certain Mannich Bases of 2-ethoxycarbonylindoles and 5 H-pyridazino [4, 5-b] indoles. *Archives of Pharmacol Research*, 2001. 24: p. 21-26.
 - Buravlev, E.V., et al., Novel Mannich bases of α - and γ -mangostins: synthesis and evaluation of antioxidant and membrane-protective activity. *European journal of medicinal chemistry*, 2018. 152: p. 10-20.
 - Abdel-Rahman, I.M., et al., Novel Mannich bases of ciprofloxacin with improved physicochemical properties, antibacterial, anticancer activities and caspase-3 mediated apoptosis. *Bioorganic Chemistry*, 2021. 107: p. 104629.
 - M Patel, H., K. D Patel, and H. D Patel, Facile synthesis and biological evaluation of New Mannich products as potential antibacterial, antifungal and antituberculosis agents: molecular docking study. *Current Bioactive Compounds*, 2017. 13(1): p. 47-58.
 - Kalaivanan, C., et al., Novel Cu (II) and Ni (II) complexes of nicotinamide based Mannich base: Synthesis, characterization, DFT calculation, DNA binding, molecular docking, antioxidant, antimicrobial activities. *Journal of Molecular Liquids*, 2020. 320: p. 114423.
 - Zulfareen, N., et al., Adsorption and quantum chemical studies on the inhibition potential of Mannich base for the corrosion of brass in acid medium. *Arabian Journal for Science and Engineering*, 2017. 42(1): p. 125-138.
 - Al-Shammari, A.M., et al., In vitro synergistic enhancement of Newcastle Disease Virus to 5-fluorouracil cytotoxicity against tumor cells. *Biomedicines*, 2016. 4(1): p. 3.
 - Liu, Y., et al., Synthesis of novel ferrocenyl Mannich bases and their antibacterial activities. *Journal of Molecular Structure*, 2018. 1157: p. 482-485.
 - Spinu, C. and A. Kriza, Co (II), Ni (II) and Cu (II) complexes of bidentate Schiff bases. *Acta Chimica Slovenica*, 2000. 47(2): p. 179-186.
 - Yousef, T.A., G.M. Abu El-Reash, and R.M. El Morshedy, Structural, spectral analysis and DNA studies of heterocyclic thiosemicarbazone ligand and its Cr(III), Fe(III), Co(II) Hg(II), and U(VI) complexes. *Journal of Molecular Structure*, 2013. 1045: p. 145-159.
 - Panchal, P., et al., Coordination Polymeric Assemblies of some d-Block Elements with Schiff Bases and its Characterization. *Journal of Macromolecular Science, Part A: Pure and Applied Chemistry*, 2007. 44(4): p. 373-378.
 - Shupack, S., et al., The electronic structures of square-planar metal complexes. V. Spectral properties of the maleonitriledithiolate complexes of nickel, palladium, and platinum. *Journal of the American Chemical Society*, 1964. 86(21): p. 4594-4602.
 - Bosnich, B., An interpretation of the circular dichroism and electronic spectra of salicylaldehyde complexes of square-coplanar diamagnetic nickel (II). *Journal of the American Chemical Society*, 1968. 90(3): p. 627-632.
 - Jeslin Kanaga Inba, P., et al., Cu (II), Ni (II), and Zn (II) complexes of salan-type ligand containing ester groups: synthesis, characterization, electrochemical properties, and in vitro biological activities. *Bioinorganic chemistry and applications*, 2013. 2013.

30. Mohod, R., Synthesis, characterization and thermal studies of 1-substituted-3-formamidinothiocarbamides Complexes. 2018.
31. Lever, A.P., Inorganic electronic spectroscopy. Studies in physical and theoretical chemistry, 1984. 33.
32. Rush, R.M., D.S. Martin, and R.G. LeGrand, Polarized crystal spectra of potassium tetrachloropalladate (II) and potassium tetrabromopalladate (II). Inorganic Chemistry, 1975. 14(10): p. 2543-2550.
33. Sekhar, E.V., K. Jayaveera, and S. Srihari, Synthesis and characterization of metal complexes of 4-((furan-2-ylmethylene) amino) benzene sulfonamide. IOSR J. Appl. Chem. Ver. I., 2015. 8: p. 42-45.
34. Mostafa MH, K., et al., Synthesis and characterization of a novel schiff base metal complexes and their application in determination of iron in different types of natural water. Open Journal of Inorganic Chemistry, 2012. 2012.
35. Jørgensen, C.K., Absorption spectra and chemical bonding in complexes. 2015: Elsevier.
36. Figgis, B.N. and I. Goodman, Introduction to ligand fields. 1966: Interscience publishers.
37. Rasheed, R.T., Synthesis of new metal complexes derived from 5-nitroso 8-hydroxy quinoline and Salicylidene P-imino acetophenone with Fe (II), Co (II), Ni (II) and Cu (II) ions. Journal of Al-Nahrain University, 2012. 15(4): p. 68-73.
38. Tiera, M.J., et al., Synthesis and characterization of phosphorylcholine-substituted chitosans soluble in physiological pH conditions. Biomacromolecules, 2006. 7(11): p. 3151-3156.
39. Abdel-Aziz, M., et al., Novel N-4-piperazinyl-ciprofloxacin-chalcone hybrids: synthesis, physicochemical properties, anticancer and topoisomerase I and II inhibitory activity. European journal of medicinal chemistry, 2013. 69: p. 427-438.
40. Chen, D., et al., Inhibition of prostate cancer cellular proteasome activity by a pyrrolidine dithiocarbamate-copper complex is associated with suppression of proliferation and induction of apoptosis. Front Biosci, 2005. 10(2): p. 2932-9.
41. Sun, R.W.-Y., et al., Some uses of transition metal complexes as anti-cancer and anti-HIV agents. Dalton Transactions, 2007(43): p. 4884-4892.
42. Abdnoor, Z.M. and A.J. Alabdali, Synthesis, characterization, and anticancer activity of someazole-heterocyclic complexes with gold (III), palladium (II), nickel (II), and copper (II) metal ions. Journal of the Chinese Chemical Society, 2019. 66(11): p. 1474-1483.
43. Tugrak, M., et al., Synthesis of mono Mannich bases of 2-(4-hydroxybenzylidene)-2, 3-dihydroinden-1-one and evaluation of their cytotoxicities. Journal of Enzyme Inhibition and Medicinal Chemistry, 2016. 31(5): p. 818-823.